

# 000 BENCHMARKING LARGE VISION-LANGUAGE MODELS 001 ON FINE-GRAINED IMAGE TASKS: A COMPREHENSIVE 002 EVALUATION 003

004 **Anonymous authors**  
005  
006

007 Paper under double-blind review  
008  
009

## 010 ABSTRACT 011

012  
013 Recent advancements in Large Vision-Language Models (LVLMs) have demon-  
014 strated remarkable multimodal perception capabilities, garnering significant at-  
015 tention. While numerous evaluation studies have emerged, assessing LVLMs  
016 both holistically and on specialized tasks, fine-grained image tasks—fundamental  
017 to computer vision—remain largely unexplored. To fill this gap, we introduce  
018 a comprehensive fine-grained evaluation benchmark, *i.e.*, FG–BMK, comprising  
019 1.01 million questions and 0.28 million images. Our evaluation systematically  
020 examines LVLMs from both human-oriented and machine-oriented perspectives,  
021 focusing on their semantic recognition and fine-grained feature representation ca-  
022 pabilities. Through extensive experiments on twelve representative LVLMs/VLMs,  
023 we uncover key findings regarding the influence of training paradigms, modality  
024 alignment, perturbation susceptibility, and fine-grained category reasoning on task  
025 performance. This work provides critical insights into the limitations of current  
026 LVLMs and offers guidance for future data construction and model design in the  
027 development of more advanced LVLMs. Our code is open-source and available at  
028 <https://anonymous.4open.science/r/FG-BMK-7B51>.  
029

## 030 1 INTRODUCTION 031

032 Large language models have recently achieved remarkable advancements, with models like GPT-  
033 4 (OpenAI, 2023) surpassing human-level performance across diverse tasks. Building on this, Large  
034 Vision-Language Models (LVLMs) have rapidly evolved, with models such as GPT-4o (OpenAI,  
035 2023), Qwen (Bai et al., 2023), InternVL (Chen et al., 2024), and LLaVA-1.5 (Liu et al., 2024a)  
036 demonstrating strong multimodal reasoning and perception capabilities.  
037

038 In response to these advancements, various holistic and specialized evaluations have emerged to  
039 assess the capabilities of LVLMs. For instance, LVLM-eHub (Xu et al., 2025) and MMBench (Yuan  
040 et al., 2024) provide broad evaluations of multimodal perception and reasoning, while specialized  
041 evaluations like DocVQA (Mathew et al., 2021) and GQA (Hudson & Manning, 2019) focus on  
042 specific tasks, such as document visual perception and visual reasoning. While these evaluations have  
043 provided valuable insights, a critical gap remains: there is no systematic evaluation of LVLMs on  
044 fine-grained image tasks, which focus on analyzing visual objects at the subordinate category level  
045 and are fundamental to computer vision (Wei et al., 2022b). Consequently, the capability boundaries  
046 of LVLMs in fine-grained tasks remain poorly understood.

047 To address this gap, we propose a comprehensive fine-grained evaluation benchmark, termed FG–BMK.  
048 This benchmark includes 1.01 million questions and 0.28 million images, providing a robust test  
049 bed for evaluating LVLMs. FG–BMK incorporates two evaluation paradigms: human-oriented and  
050 machine-oriented. The human-oriented evaluation employs dialogue-like interactions to assess a  
051 model’s ability to understand and respond to fine-grained visual queries in a conversational context.  
052 The machine-oriented evaluation focuses on two core fine-grained vision tasks—image retrieval and  
053 recognition—to directly measure the feature representation capabilities of LVLMs. Together, these  
054 evaluations enable a comprehensive assessment of LVLMs’ fine-grained feature representation and  
055 semantic recognition abilities.

054 Through extensive evaluations across representative LVLMs and VLMs within FG-BMK, we derive  
 055 several key insights:  
 056

- 057 • The contrastive training paradigm in LVLMs proves more effective in enhancing the fine-grained  
 058 discriminability of visual features, whereas generative and reconstruction-based training paradigms  
 059 tend to yield weaker discriminability.
- 060 • Aligning visual features with textual features in LVLMs can impair their fine-grained discrim-  
 061 inability, particularly when there is a mismatch in granularity between the paired image-text  
 062 data.
- 063 • LVLMs and LVMs are more vulnerable to feature perturbations in fine-grained tasks than in generic  
 064 vision tasks.
- 065 • LVLMs demonstrate relatively stronger capabilities in perceiving visual appearances but face chal-  
 066 lenges in fine-grained category reasoning (which depends on the recognition of visual attributes).
- 067 • Despite their advancements, LVLMs still lag behind fine-grained tailored models in handling  
 068 fine-grained visual tasks.

069 These findings provide a foundation for future research aimed at advancing LVLM performance in  
 070 fine-grained tasks and addressing the challenges uncovered by FG-BMK.

## 072 2 RELATED WORK

074 **Large Vision-Language Models** Large Language Models (LLMs) like GPT-4 (OpenAI, 2023) have  
 075 made notable strides in text comprehension, reasoning, and generation. Building on this foundation,  
 076 Large Vision-Language Models (LVLMs) have emerged with impressive reasoning and perception  
 077 abilities across diverse tasks. Enhancing LVLM performance has taken various directions: BLIP (Li  
 078 et al., 2022) uses noisy web data with bootstrapped captions; LLaVA (Liu et al., 2024a) employs  
 079 GPT-4-generated instruction-following data; BLIP-2 (Li et al., 2023) integrates frozen image and  
 080 text encoders; Qwen2.5-VL (Bai et al., 2023) leverages dynamic-resolution strategy for preserving  
 081 native image resolution; InternVL3 (Zhu et al., 2025) unifies pre-training over multimodal data for  
 082 improved effectiveness. While achieving success on many tasks, fine-grained visual challenges for  
 083 these LVLMs remain underexplored. This work addresses this gap by assessing their performance in  
 084 fine-grained domains, uncovering both their potential and limitations.

085 **Large Vision-Language Model Benchmarks** While LVLMs have shown impressive performance,  
 086 various benchmarks have been developed to evaluate their capabilities in different domains. Special-  
 087 ized benchmarks like ChartQA (Masry et al., 2022) for chart understanding, DocVQA (Mathew et al.,  
 088 2021) for document visual perception, and GQA (Hudson & Manning, 2019) for visual reasoning  
 089 provide focused assessments. Additionally, evaluations in optical character recognition (Liu et al.,  
 090 2024b) and adversarial robustness (Madry et al., 2018) offer insights into specialized aspects of LVLM  
 091 performance. Holistic evaluations, such as LVLM-eHub (Xu et al., 2025) and MMBench (Yuan et al.,  
 092 2024), assess general multimodal perception and reasoning, while others like MathVista (Lu et al.,  
 093 2024) and MMMU (Yue et al., 2024) include expert-level problems spanning multiple disciplines.

094 However, comprehensive evaluations of LVLMs in fine-grained visual tasks remain scarce. Existing  
 095 efforts, such as (Geigle et al., 2024), primarily focus on fine-grained classification, and (Zhang  
 096 et al., 2024) evaluates classification and reasoning with limited questions. To address it, we pro-  
 097 pose FG-BMK, a benchmark designed to comprehensively evaluate LVLMs' fine-grained feature  
 098 representation and semantic recognition capabilities across diverse visual tasks.

099 **Fine-Grained Image Tasks** Fine-grained visual tasks (Wei et al., 2022b; Xu et al., 2022; Wei  
 100 et al., 2024; Wu et al., 2024; Jing et al., 2024a; Zhang & Hou, 2024) are pivotal in applications  
 101 like biodiversity monitoring (Jing et al., 2024b), object retrieval (Shen et al., 2022), and product  
 102 recommendation (Wei et al., 2022a). While LVLMs such as GPT-4, InternVL, and Qwen excel  
 103 in tasks like OCR, visual question answering, and image captioning, fine-grained tasks remain a  
 104 significant challenge. These tasks demand models to identify subtle, discriminative patterns in  
 105 images (Song et al., 2020) and leverage expert knowledge from LLMs for precise responses. To  
 106 address this, we introduce a comprehensive benchmark and conduct extensive experiments to evaluate  
 107 LVLMs' performance on fine-grained tasks. Our study systematically highlights their limitations and  
 offers actionable insights for advancing model design and training.

Human-oriented Evaluation																				
<b>Attribute Recognition</b>	<b>Knowledge Bias Estimation</b>	<b>Hierarchical Granularity Recognition:</b>																		
<p><b>Q:</b> What is the eye color of the bird in this image? Choose one answer from the following list: [blue, <b>black</b>, ..., red, rufous]</p> <p><b>Q:</b> Is the eye color of the bird in this image black?</p> <p>Type :   </p>	<p><b>Q<sub>P</sub>:</b> From your observation, is the species of the dog shown a Chihuahua? Yes</p> <p><b>Q<sub>N</sub>:</b> Does this dog belong to the species known as japanese spainel? No</p> <p>Type :  </p>	<p><b>Class:</b> Is the class of the object aves?</p> <p><b>Genus:</b> What is the genus of the object? [auklet, cormorant, bunting, <b>towhee</b>]</p> <p><b>Species:</b> What is the species of the object?</p> <p>Type:   </p>																		
Machine-oriented Evaluation																				
<b>Image Retrieval</b> <p>Gallery Image:       Cosine Similarity Between Query Set: {</p> <table> <tr> <td></td> <td>: 0.8956</td> </tr> <tr> <td></td> <td>: 0.7942</td> </tr> <tr> <td></td> <td>: 0.7542</td> </tr> <tr> <td></td> <td>: 0.6952</td> </tr> <tr> <td>...</td> <td></td> </tr> <tr> <td>Query Image: </td> <td>: 0.5978</td> </tr> </table> <p>Input: Image      Output: Image Similarity      Metric: mAP</p>		: 0.8956		: 0.7942		: 0.7542		: 0.6952	...		Query Image:	: 0.5978	<b>Image Classification</b> <p>GT: Gulfstream IV      Predicted Class Probability: {</p> <table> <tr> <td>Gulfstream IV: 0.75</td> <td>Gulfstream V: 0.20</td> </tr> <tr> <td>...</td> <td>Falcon 2000: 0.01</td> </tr> <tr> <td>(Within Meta-class)</td> <td>(Across Meta-class)</td> </tr> </table> <p>Input: Image      Output: Class Probability      Metric: Top-1 Acc</p>	Gulfstream IV: 0.75	Gulfstream V: 0.20	...	Falcon 2000: 0.01	(Within Meta-class)	(Across Meta-class)	
	: 0.8956																			
	: 0.7942																			
	: 0.7542																			
	: 0.6952																			
...																				
Query Image:	: 0.5978																			
Gulfstream IV: 0.75	Gulfstream V: 0.20																			
...	Falcon 2000: 0.01																			
(Within Meta-class)	(Across Meta-class)																			

Figure 1: Our proposed benchmark: The human-oriented evaluation tests the model’s ability to handle fine-grained visual queries (true/false, multiple-choice, short-answer), while the machine-oriented evaluation directly assesses visual feature representation through image retrieval and classification tasks. =true/false question, =multiple-choice question, =short-answer question.

### 3 THE EVALUATION BENCHMARK

#### 3.1 EVALUATION TASKS AND METRICS

To comprehensively evaluate LVLMs, we adopt two evaluation paradigms: 1) *human-oriented evaluation* and 2) *machine-oriented evaluation*.

Specifically, since dialogue is the most direct way for humans to interact with LVLMs, the human-oriented evaluation assesses the model’s ability to understand and respond to fine-grained visual queries in a conversational setting. We utilize three types of questions—true/false, multiple-choice, and short-answer (cf. Figure 1)—where a response is considered correct if it includes the ground truth.

While, the machine-oriented evaluation encompasses two fundamental vision tasks (Wei et al., 2022b): image retrieval and image classification. To evaluate the feature representation ability of LVLMs, we measure the accuracy of their visual features on these tasks. Following the DINOv2 approach (Oquab et al., 2023), we use mean Average Precision (mAP) for retrieval and Top-1 accuracy for classification.

The detailed aspects of both human-oriented and machine-oriented evaluations are outlined below:

#### Human-oriented Evaluation:

- **Attribute Recognition:** This includes true/false questions and multiple-choice questions, designed to evaluate the model’s ability to identify visual attributes such as size, color, length, shape, pattern, and more.
- **Knowledge Bias Estimation:** This section consists exclusively of true/false questions, designed to uncover potential knowledge biases across different fine-grained categories by evaluating LVLM’s accuracy for each category.
- **Hierarchical Granularity Recognition:** This section includes true/false questions, multiple-choice questions, and short-answer questions, designed to evaluate the LVLMs’ ability to leverage domain-specific knowledge to identify object categories in images across different levels of granularity within hierarchical taxonomies.

#### Machine-oriented Evaluation:

- **Image Retrieval:** retrieves images belonging to multiple subordinate categories of a meta-category by measuring the similarity of their visual features.

162 • *Image Classification*: recognizes images into fine-grained categories, either within a single meta-  
 163 category (e.g., species of animals, models of cars) or across multiple meta-categories, assessing the  
 164 model’s ability to handle diverse data sources and make accurate predictions.

165 More evaluation tasks details are presented in Appendix A.1.

167 **3.2 DATA CURATION**

169 To ensure the quality and diversity of the data, we source images for the FG-BMK benchmark from  
 170 12 well-established fine-grained datasets, which helps avoid issues of inconsistent image quality and  
 171 the risk of mislabeling often found in web-sourced images (Radford et al., 2021).

172 • *Attribute Recognition*: We design true/false and multiple-choice questions based on the fine-grained  
 173 annotations of the images. For the multiple-choice questions, the options include all possible  
 174 attribute candidates. In contrast, for the true/false questions, half are negative samples, pairing the  
 175 image with an incorrect attribute, and the other half are positive samples.

176 • *Knowledge Bias Estimation*: In addition to positive samples, for each fine-grained category label,  
 177 we pair it with images from other subcategories within the same super-category to generate negative  
 178 samples for true/false questions.

179 • *Hierarchical Granularity Recognition*: We design true/false, multiple-choice, and short-answer  
 180 questions at various levels of granularity based on the hierarchical taxonomy labels of the images.  
 181 For true/false questions, negative samples are created by pairing images with incorrect labels  
 182 at the same hierarchical level (e.g., an image of Aves (birds) paired with Insecta (insects)). For  
 183 multiple-choice questions, options are drawn from different categories within the same parent  
 184 category of the hierarchical taxonomy (e.g., species-level options such as black-footed albatross  
 185 and Laysan albatross, both within the genus Albatross). For short-answer questions, the model is  
 186 prompted to generate its response directly.

187 • *Image Retrieval and Classification*: We use the original labels directly from the datasets. For  
 188 classification across meta-categories, we combine subcategories from different meta-categories  
 189 into a unified training/testing set, where all fine-grained categories are mixed for training.

190 More specifically, for each task in the human-oriented evaluation, we manually design several  
 191 question templates to ensure both diversity and comprehensive coverage. More details of curated  
 192 data can be found in Appendix A.2.

194 **4 OBSERVATIONS AND DISCUSSIONS**

196 **4.1 MODELS UNDER EVALUATION**

198 Given the diverse landscape of existing LVLMs, we select nine widely-used open-source LVLMs, two  
 199 closed-source models (GPT-4o-1120 (OpenAI, 2023) and Gemini-2.0-flash (Gemini Team, 2024))  
 200 and one purely visual model with varying training strategies, as shown in Table 1. To enable clear  
 201 comparisons and isolate the factors influencing performance, we use earlier versions of models from  
 202 each family in machine-oriented evaluation, where their distinct characteristics are more evident  
 203 and less affected by additional tricks or complex modifications. Further details about the evaluated  
 204 models can be found in Appendix B.

205 **4.2 HUMAN-ORIENTED EVALUATION**

207 In the human-oriented evaluation, we assess the ability of LVLMs to understand visual content and  
 208 utilize domain-specific knowledge through conversational interactions. Specifically, we first evaluate  
 209 the domain-specific knowledge embedded in LVLMs by measuring their accuracy in identifying  
 210 object categories across different levels of granularity, as illustrated in Figure 2. Then, we investigate  
 211 whether LVLMs exhibit knowledge biases when recognizing different fine-grained categories by  
 212 ranking their accuracy in answering true/false questions for each category, cf. Figure 3. Additionally,  
 213 we examine the capability of LVLMs to recognize fine-grained attributes, with results summarized  
 214 in Table 2. Lastly, Table 3 compares the classification accuracy of LVLMs against state-of-the-art  
 215 fine-grained tailored models on datasets spanning various domains. Based on these observations, we  
 draw the following conclusions.

Table 1: Training strategies of the open-source evaluated models. “DINOv2” is a purely visual model. “Con” denotes contrastive loss, “Gen” generative loss, “Mat” image-text matching loss, “Rec” reconstruction loss used in BEiT3, and “Dis” distillation loss used in DINOv2.

Model	Vision Size	Loss Function					Training Data		
		Con	Gen	Mat	Rec	Dis	< 0.1B	0.1B ~ 1B	> 1B
InternVL3-7B (Zhu et al., 2025)	ViT-L	✓	✓	✓		✓			✓
InternVL-Chat (Chen et al., 2024)	ViT-6B	✓	✓	✓					✓
LLaVA-1.5-7B (Liu et al., 2024a)	ViT-L		✓						
Qwen2.5-VL-7B (Bai et al., 2025)	ViT-600M	✓	✓	✓		✓			✓
Qwen-VL-Chat (Bai et al., 2023)	ViT-G		✓						✓
BLIP-2-XL (Li et al., 2023)	ViT-G	✓	✓	✓					
EVA-CLIP (Sun et al., 2023)	ViT-L	✓							
BEiT3 (Wang et al., 2023)	ViT-L				✓				
CoCa (Yu et al., 2022)	ViT-L	✓	✓						
DINOv2 (Oquab et al., 2023)	ViT-L	✓				✓			✓

**LVLMs struggle to distinguish excessively fine-grained categories.** As shown in Figure 2, taking InternVL3 (Zhu et al., 2025) as an example, its accuracy in answering true/false and multiple-choice questions declines as the granularity becomes finer. At the class level (e.g., “*Is the class of the object in this image an Insecta/Aves?*”), the model achieves 99.76% accuracy on multiple-choice questions and 99.77% on true/false questions.<sup>1</sup> However, as the granularity narrows to the genus level, where negative categories are drawn from different genera within the same class (e.g., “*Is the object in this image an albatross or a gull?*”), the model’s accuracy on multiple-choice questions drops to 90.75%, a decrease of 9.01%. When the granularity is further refined to the species level, where negative categories are from different species within the same genus (e.g., “*Is the object in this image a black-footed albatross/Laysan albatross?*”), the accuracy drops further to 62.48% on true/false questions and 61.18% on multiple-choice questions. This demonstrates that the model struggles to distinguish between closely related species. The results for other LVLMs exhibit similar trends to those for InternVL3. Additional examples of multiple-choice and true/false questions can be found in Appendix C.1.

**The inconsistent recognition accuracy of LVLMs across fine-grained categories can be attributed to the characteristics of their training data and the underlying LLM base.** To examine whether LVLMs exhibit knowledge bias in recognizing different fine-grained categories, we ranked their accuracy in answering true/false questions for each fine-grained category. As shown in Figure 3, using LLaVA (Liu et al., 2024a) as an example, the model demonstrates highly inconsistent recognition abilities across categories, achieving nearly 90% accuracy for some while dropping to approximately 30% for others.

We hypothesize that this inconsistency arises either from the uneven representation of fine-grained knowledge in the training data or from the inherent difficulty LVLMs face in learning certain fine-grained categories. To test this hypothesis, we fine-tuned LVLMs on datasets with balanced occurrences of fine-grained categories and evaluated their performance. As indicated by the yellow dots in Figure 3, the fine-tuned LLaVA shows consistently strong recognition ability across all fine-grained categories. It suggests that the knowledge bias is

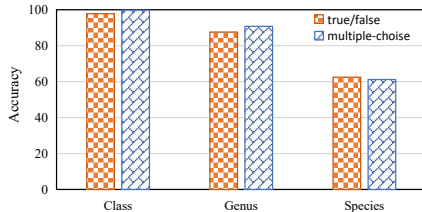


Figure 2: Results of InternVL3 (Zhu et al., 2025) on true/false and multiple-choice questions across different levels of granularity on the *CUB-200-2011* (Wah et al., 2011) dataset. The *x*-axis denotes the granularity of the recognition questions.

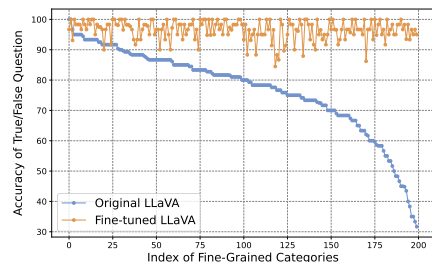


Figure 3: Comparison of the original and fine-tuned LLaVA models on occurrence-balanced fine-grained bird categories. True/false question accuracy for each category is ranked, with blue dots representing the original model and yellow dots the fine-tuned model.

<sup>1</sup>When questions are relatively simple, LVLMs achieve very high accuracy. The higher accuracy on multiple-choice questions compared to true/false questions may result from randomness.

270 Table 2: Attribute recognition accuracy of InternVL3 (Zhu et al., 2025) on the *CUB-200-2011* (Wah  
 271 et al., 2011) dataset (values in parentheses represent the average accuracy for each attribute).

Color Attribute (47.40)							
belly color	58.49	back color	34.98	bill color	51.31	breast color	54.25
crown color	55.30	eye color	84.59	forehead color	53.32	leg color	44.01
nape color	39.24	throat color	52.77	under tail color	34.69	underparts color	56.20
upper tail color	37.30	upperparts color	28.75	wing color	30.16	primary color	43.05
Pattern Attribute (50.13)							
back pattern	40.94	belly pattern	68.13	breast pattern	65.12	head pattern	35.92
tail pattern	41.64	wing pattern	49.04				
Shape Attribute (30.95)							
bill shape	37.61	shape	52.37	tail shape	10.42	wing shape	23.39
Length Attribute (71.03)				Size Attribute (52.55)			
bill length			71.03	size			52.55

285 primarily caused by the uneven representation of fine-grained knowledge in training data, rather than  
 286 the inherent difficulty of learning specific categories.

288 To further validate this hypothesis, we examined the occurrence frequency of fine-grained categories  
 289 in the LVLM’s training data. Interestingly, we found that such categories are almost absent from the  
 290 training data. This indicates that the observed inconsistency in recognition ability is inherited from  
 291 the language model underlying the LVLM, rather than being solely a consequence of the visual model  
 292 itself. Additional results for other LVLMs exhibit similar trends and can be found in Appendix C.2.

294 **LVLMs exhibit significant room for improvement in recognizing fine-grained attributes.** As  
 295 shown in Table 2 of the paper and Table 12 in the appendix, LVLMs exhibit relatively stronger  
 296 recognition abilities for attributes like pattern, size and length compared to others. For example,  
 297 InternVL3 (Zhu et al., 2025) and Qwen2.5-VL (Bai et al., 2025) achieve 50.13% and 45.12% average  
 298 accuracy for pattern recognition, but only 30.95% and 29.30% for shape recognition. Notably, only  
 299 a few attributes achieved an accuracy above 70%, and several attributes scored as low as 10%,  
 300 highlighting significant room for improvement in LVLMs’ fine-grained attribute recognition.

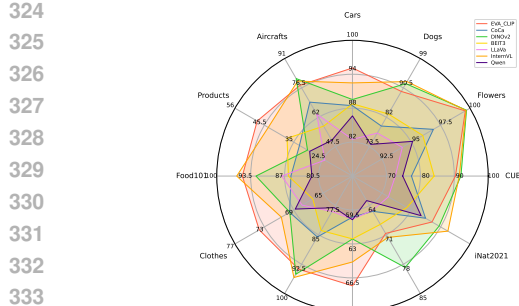
301 We also observe model-specific differences in attribute recognition. For instance, while InternVL3  
 302 struggles more with pattern recognition compared to size, Gemini-2.0-flash (Gemini Team, 2024)  
 303 shows the opposite trend. Additionally, we find that the latest LVLMs show significant improvements  
 304 in pattern and length recognition, while their advancements in color and shape recognition are more  
 305 limited. Detailed results of the attribute recognition task are provided in Appendix C.3.

306 **LVLMs do not outperform fine-grained  
 307 tailored models in fine-grained tasks.**  
 308 In Table 3, we compare the recognition accuracy of LVLMs with that of fine-grained tailored  
 309 models. While LVLMs demonstrate notable performance in fine-grained  
 310 recognition, their accuracy—whether in  
 311 short-answer questions or using the linear  
 312 classifier method—falls short of that  
 313 achieved by fine-grained tailored models.  
 314 This disparity may stem from the fact that  
 315 LVLMs are primarily optimized for general  
 316 tasks, with less emphasis placed on  
 317 fine-grained domain capabilities (e.g., CAP (Behera et al., 2021) uses context-aware attentional  
 318 pooling to capture hierarchical contextual information from pixel to region to image level, leading to  
 319 a 1.53% improvement in classification accuracy).

322 Due to the architectural paradigm of LVLMs (typically ViT + MLP + LLM), these components  
 323 cannot be directly applied. However, the core idea of attending to hierarchical-level details can  
 324 still be incorporated into LVLMs (e.g., InternVL3 (Zhu et al., 2025) not only takes the full image

326 Table 3: Comparison of LVLMs and fine-grained tailored  
 327 models on classification tasks. “SA” denotes LVLM re-  
 328 sults fine-tuned on fine-grained datasets for short-answer  
 329 questions, “LC” represents linear classifier results us-  
 330 ing LVLM visual features, and “FG-Tailored” refers to  
 331 state-of-the-art fine-grained tailored model results.

Datasets	SA	LC	FG-Tailored
<i>CUB-200-2011</i>	85.60	91.65	93.10 (Diao et al., 2022)
<i>Stanford Dog</i>	86.49	90.50	97.30 (Bera et al., 2022)
<i>Stanford Car</i>	90.55	94.30	97.10 (Liu, 2024)
<i>Food-101</i>	95.25	95.67	98.60 (Behera et al., 2021)
<i>FGVC Aircraft</i>	66.19	78.88	95.40 (Sikdar et al., 2024)



324  
325  
326  
327  
328  
329  
330  
331  
332  
333  
334  
335  
336  
337  
338  
339  
340  
341  
342  
343  
344  
345  
346  
347  
348  
349  
350  
351  
352  
353  
354  
355  
356  
357  
358  
359  
360  
361  
362  
363  
364  
365  
366  
367  
368  
369  
370  
371  
372  
373  
374  
375  
376  
377  
Figure 4: Retrieval results of LVLM visual features on twelve fine-grained datasets. Different colors represent different models.

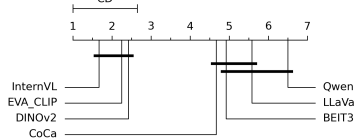


Figure 6: Nemenyi statistical test results for fine-grained retrieval. Black horizontal lines indicate the critical distance (CD), grouping models with no significant performance differences.

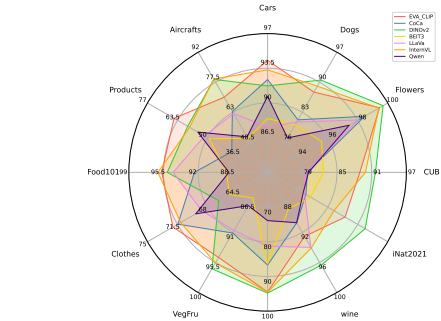


Figure 5: Classification results of LVLM visual features on twelve fine-grained datasets. Different colors represent different models.

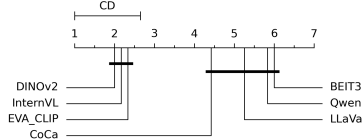


Figure 7: Nemenyi statistical test results for fine-grained recognition. Black horizontal lines indicate the critical distance (CD), grouping models with no significant performance differences.

as input, but also divides the image into parts to obtain more fine-grained visual representations). Enhancing LVLMs performance in specialized areas (*e.g.*, fine-grained recognition) while preserving their strengths in general tasks presents an important and promising direction for future research.

#### 4.3 MACHINE-ORIENTED EVALUATION

Compared to human-oriented evaluation, machine-oriented evaluation takes a more direct approach to assess the visual feature representations of LVLMs by employing two fundamental visual tasks: image retrieval and image recognition. This evaluation focuses on two key aspects: 1) Discriminability—the ability of visual features to distinguish fine-grained categories, and 2) Robustness—maintaining accuracy under feature perturbations.

To evaluate discriminability, we start by analyzing the performance of visual features on retrieval and classification tasks, following the setting of DINOv2 (Oquab et al., 2023). Figures 4 and 5 display retrieval and classification results across twelve fine-grained datasets, while Figures 6 and 7 provide the Friedman test results for these tasks.

We then increase classification difficulty by merging fine-grained categories from different super-categories into a unified training and testing set. Figure 8 presents classification accuracy within a single super-category and across multiple meta-categories. Visual features with strong discriminability should maintain high accuracy even with diverse data sources. Additionally, we analyze how the vision encoder size in LVLMs impacts classification accuracy, as shown in Figure 9.

Furthermore, we examine how vision-language alignment—a critical component of LVLMs—affects visual feature quality. Specifically, we compare classification accuracy between original visual features and those aligned to textual features in fine-grained classification tasks, as shown in Table 4.

To investigate robustness, we introduce perturbations to visual features using projected gradient descent (Madry et al., 2018) and analyze their impact on classification accuracy. Results of this experiment are presented in Table 5.

**The contrastive training paradigm in LVLMs effectively enhances the fine-grained discriminability of visual features.** In Figure 4 and Figure 5, vision encoders trained with contrastive paradigms (*e.g.*, EVA-CLIP, InternVL, DINOv2) outperform those trained with reconstruction (BEiT3) and generative paradigms (Qwen) on fine-grained retrieval and classification tasks. As

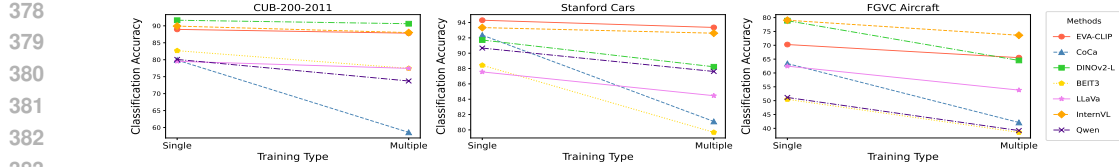


Figure 8: Classification results of LVLM visual features on fine-grained datasets. “Single” denotes accuracy from training on a single meta-category, while “Multiple” reflects accuracy from training on a unified dataset combining multiple meta-categories.

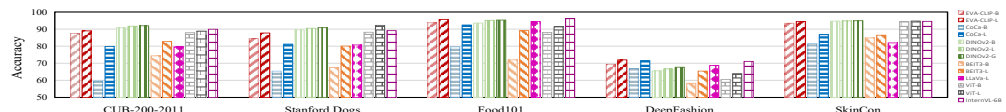


Figure 9: Classification results with different vision encoder sizes. Bars filled with different patterns represent different models, with darker patterns indicating larger vision encoder sizes.

shown in Figure 6 and Figure 7, Nemenyi test results also indicate that InternVL, EVA-CLIP, and DINOv2 perform significantly better than Qwen and BEiT3. In multi meta-category classification (cf. Figure 8), EVA-CLIP maintains high accuracy, with an average drop of just 1.96% compared to the single-category setting, while Qwen and BEiT3 show larger drops of 4.16% and 7.41%, respectively. This underscores the effectiveness of contrastive paradigms in fine-grained tasks.

In experiments of vision encoder size, as shown in Figure 9, we observe that DINOv2-B, with a smaller vision encoder, achieves higher classification accuracy compared to BEiT3-L, with a larger vision encoder, outperforming by 8.08% on *CUB-200-2011* and 9.49% on *Stanford Dogs*. We attribute these findings to the limitations of generative and reconstruction training paradigms, which fail to adequately distinguish between features of different fine-grained categories, while maintaining similarity within the same. This limitation hinders their performance on fine-grained tasks.

**The alignment strategy in LVLMs might impair the fine-grained discriminability of visual features.** Alignment plays a critical role in LVLMs by bridging the gap between visual and textual features. To assess its impact on fine-grained visual feature discriminability, we compare the classification accuracy of LLaVA’s (Liu et al., 2024a) original visual features with those aligned to textual features on fine-grained classification tasks. As shown in the first two columns of Table 4, the original features demonstrate superior classification performance, outperforming the aligned ones by an average of 3.39%.

This decline in performance can be attributed to two key factors. First, aligning visual and textual features may introduce distortions due to inconsistencies between their respective feature spaces. Second, granularity inconsistencies in LVLMs’ alignment data—where fine-grained objects in images are paired with coarse-grained textual descriptions (as demonstrated in our qualitative analysis in Appendix D.1)—negatively affect the discriminability of the aligned visual features.

To validate the impact of granularity inconsistency, we construct a new alignment dataset where the textual descriptions match the granularity of the fine-grained objects in images. We then retrain the alignment module in LLaVA using this dataset. As shown in Table 4, the classification accuracy of visual features aligned with fine-grained textual content improves significantly, with an increase of 2.55% on *Stanford Dogs* and 1.73% on *Stanford Cars*. While the aligned visual features still underperform compared to the original features, these results underscore the detrimental effects of granularity inconsistency on visual feature discriminability and highlight the importance of ensuring granularity alignment between image and textual content. Further experiments in Appendix D.2 reveal that enhancing the fine-grained discriminability of visual features during the alignment stage can lead to improved LVLM performance on fine-grained tasks.

Table 4: Classification accuracy of LLaVA visual features before and after alignment. “Origin” denotes original features from the vision encoder. “Aligned” denotes features aligned to text with inconsistent granularity, while “Aligned-FG” denotes those aligned to fine-grained text.

Datasets	Origin	Aligned	Aligned-FG
<i>CUB-200-2011</i>	79.77	73.17	75.06
<i>Stanford Dogs</i>	81.24	78.14	80.69
<i>Stanford Cars</i>	87.57	83.90	85.63
<i>Food-101</i>	94.27	93.35	94.32
<i>DeepFashion</i>	69.94	67.30	67.75

432  
 433 Table 5: Classification results of LVLMs’ original and perturbed visual features on the fine-grained  
 434 dataset *CUB-200-2011* and the generic dataset *CIFAR-100*. “Origin” refers to results with original  
 435 features, while “Perturbed” indicates results with perturbed features.

Datasets	EVA-CLIP		CoCa		DINOv2		ViT	
	Origin	Perturbed	Origin	Perturbed	Origin	Perturbed	Origin	Perturbed
<i>CIFAR-100</i>	93.05	50.76	86.94	52.23	93.38	42.39	89.81	72.15
<i>CUB-200-2011</i>	88.95	24.94	79.89	23.40	91.64	25.94	88.83	73.85

436  
 437  
 438  
 439  
 440 **Larger vision encoder size or larger scale of web data provides limited improvement in the**  
 441 **fine-grained discriminability of visual features.** Regarding vision encoder size, as shown in  
 442 Figure 9, increasing the size of DINOv2’s vision encoder from DINOv2-B to DINOv2-L results in  
 443 only a 0.6% improvement in average classification accuracy, while further increasing from DINOv2-L  
 444 to DINOv2-G leads to just a 0.3% improvement. The classification accuracy of visual features in  
 445 InternVL-6B is not superior to that of DINOv2-L, suggesting that merely enlarging the vision encoder  
 446 has limited impact on enhancing the fine-grained discriminability of visual features.  
 447

448 Regarding the amount of training data, as shown in Figure 7, the vision encoder of EVA-CLIP,  
 449 trained on over 2 billion data samples, does not outperform DINOv2, which was trained on 142  
 450 million samples, in fine-grained classification and retrieval tasks. We attribute this difference to the  
 451 quality of the training data, that DINOv2’s dataset is carefully curated from a large pool of data,  
 452 whereas EVA-CLIP relies on crawled web data. A similar trend is observed when comparing DINOv2  
 453 with InternVL (6B samples), suggesting that simply increasing the scale of training data, without  
 454 considering its quality, offers limited improvement in fine-grained discriminability of visual features.  
 455

456 **Visual features in LVLMs are more susceptible to perturbations in fine-grained tasks.** As  
 457 shown in Table 5, perturbing the visual features of EVA-CLIP causes a significant drop in classification  
 458 accuracy on the fine-grained dataset *CUB-200-2011* (from 88.95% to 24.94%). In contrast, on the  
 459 generic dataset *CIFAR-100* (Krizhevsky & Hinton, 2009), the accuracy declines more modestly (from  
 460 93.05% to 50.76%). Similar trends are observed for CoCa and DINOv2, indicating that fine-grained  
 461 tasks are more susceptible to perturbations than generic tasks. We attribute this vulnerability to coarse-  
 462 grained, noisy training data, which limits feature discriminability across fine-grained categories,  
 463 making it hard to distinguish them when visual features are perturbed.  
 464

465 In contrast, the Vision Transformer (Wightman, 2019) trained on the *ImageNet* (Deng et al., 2009)  
 466 dataset with cross-entropy loss demonstrates superior robustness to perturbations. It shows only  
 467 minor declines in classification accuracy on both fine-grained and generic datasets. This suggests that  
 468 adopting alternative training paradigms or incorporating high-quality, fine-grained data (as seen in  
 469 *ImageNet*) during training could help improve the robustness of visual features in LVLMs.  
 470

## 5 CONCLUDING REMARKS

471 We conducted a comprehensive evaluation to investigate the capabilities of LVLMs on fine-grained  
 472 visual tasks, leading to several key findings. First, we observed that the contrastive training paradigm  
 473 significantly enhances the fine-grained discriminability of visual features, whereas generative and  
 474 reconstruction-based paradigms tend to underperform in this aspect. Second, aligning visual features  
 475 with textual features can impair their fine-grained discriminability, particularly when there is a  
 476 mismatch in granularity between the paired image-text data. Third, our experiments revealed that  
 477 LVLMs and LVMs are more susceptible to feature perturbations in fine-grained tasks compared to  
 478 generic vision tasks, highlighting a vulnerability that merits further attention. Fourth, while LVLMs  
 479 demonstrate strong capabilities in visual appearance perception, they face notable challenges in fine-  
 480 grained category reasoning, which depends heavily on recognizing subtle visual attributes. Finally,  
 481 despite their advancements, LVLMs still lag behind specialized fine-grained models, underscoring the  
 482 need for task-specific enhancements. These findings highlight key limitations of LVLMs, identifying  
 483 critical areas for improvement, such as training paradigms, robustness to perturbations, and reasoning  
 484 capabilities. Our work lays the groundwork for future research to advance LVLM performance on  
 485 fine-grained visual tasks.

486 **Ethics Statement** All data used in this study are collected from publicly available datasets that  
 487 comply with standard research ethics. The benchmark tasks and annotations in FG-BMK are con-  
 488 structed through automatic or rule-based question generation without involving human subjects.  
 489 **Although the dataset SkinCon relate to medical images, it is fully anonymized and released under**  
 490 **research-permissive licenses. Our use strictly follows its terms and involves no patient-identifying**  
 491 **information, clinical decision-making, or sensitive personal data.** We do not release any private or  
 492 sensitive information, nor do our methods introduce additional safety, fairness, or legal concerns.  
 493 Overall, FG-BMK provides a practical and ethically compliant testbed for evaluating LVLMs in  
 494 fine-grained real-world scenarios.

495 **Reproducibility Statement** We ensure reproducibility by using only publicly available datasets  
 496 and by clearly describing our benchmark construction process in Section 3 and Appendix A. The  
 497 evaluation pipeline, including prompt design, scoring methods, and model configuration, is detailed  
 498 in Section 3, Appendix A and Appendix B. We provide extensive implementation details and dataset  
 499 statistics in the Appendix. All code, data splits, and evaluation scripts has be released.  
 500

501 **REFERENCES**

503 Jinze Bai, Shuai Bai, Shusheng Yang, Shijie Wang, Sinan Tan, Peng Wang, Junyang Lin, Chang Zhou,  
 504 and Jingren Zhou. Qwen-VL: A versatile vision-language model for understanding, localization,  
 505 text reading, and beyond. *arXiv preprint arXiv:2308.12966*, 2023.

506 Shuai Bai, Keqin Chen, Xuejing Liu, Jialin Wang, Wenbin Ge, Sibo Song, Kai Dang, Peng Wang,  
 507 Shijie Wang, Jun Tang, Humen Zhong, Yuanzhi Zhu, Mingkun Yang, Zhaohai Li, Jianqiang Wan,  
 508 Pengfei Wang, Wei Ding, Zheren Fu, Yiheng Xu, Jiabo Ye, Xi Zhang, Tianbao Xie, Zesen Cheng,  
 509 Hang Zhang, Zhibo Yang, Haiyang Xu, and Junyang Lin. Qwen2.5-vl technical report. *arXiv*  
 510 *preprint arXiv:2502.13923*, 2025.

512 Yalong Bai, Yuxiang Chen, Wei Yu, Linfang Wang, and Wei Zhang. Products-10K: A large-scale  
 513 product recognition dataset. *arXiv preprint arXiv:2008.10545*, 2020.

514 Ardhendu Behera, Zachary Wharton, Pradeep RPG Hewage, and Asish Bera. Context-aware at-  
 515 tentional pooling (cap) for fine-grained visual classification. In *Proc. Conf. AAAI*, pp. 929–937,  
 516 2021.

518 Asish Bera, Zachary Wharton, Yonghuai Liu, Nik Bessis, and Ardhendu Behera. SR-GNN: Spatial  
 519 relation-aware graph neural network for fine-grained image categorization. *IEEE Trans. Image*  
 520 *Process.*, 31:6017–6031, 2022.

522 Lukas Bossard, Matthieu Guillaumin, and Luc Van Gool. Food-101–mining discriminative compo-  
 523 nents with random forests. In *Proc. Eur. Conf. Comp. Vis.*, pp. 446–461, 2014.

524 Zhe Chen, Jiannan Wu, Wenhui Wang, Weijie Su, Guo Chen, Sen Xing, Muyan Zhong, Qinglong  
 525 Zhang, Xizhou Zhu, Lewei Lu, Bin li, Ping Luo, Tong Lu, Yu Qiao, and Jifeng Dai. InternVL:  
 526 Scaling up vision foundation models and aligning for generic visual-linguistic tasks. In *Proc. IEEE*  
 527 *Conf. Comp. Vis. Patt. Recogn.*, pp. 24185–24198, 2024.

529 Roxana Daneshjou, Mert Yuksekgonul, Zhuo Ran Cai, Roberto Novoa, and James Y Zou. SkinCon:  
 530 A skin disease dataset densely annotated by domain experts for fine-grained debugging and analysis.  
 531 In *Advances in Neural Inf. Process. Syst.*, pp. 18157–18167, 2022.

532 Jia Deng, Wei Dong, Richard Socher, Li-Jia Li, Kai Li, and Li Fei-Fei. ImageNet: A large-scale  
 533 hierarchical image database. In *Proc. IEEE Conf. Comp. Vis. Patt. Recogn.*, pp. 248–255, 2009.

535 Qishuai Diao, Yi Jiang, Bin Wen, Jia Sun, and Zehuan Yuan. MetaFormer: A unified meta framework  
 536 for fine-grained recognition. *arXiv preprint arXiv:2203.02751*, 2022.

538 Gregor Geigle, Radu Timofte, and Goran Glavaš. African or european swallow? benchmarking large  
 539 vision-language models for fine-grained object classification. *arXiv preprint arXiv:2406.14496*,  
 2024.

540 Google Gemini Team. Gemini 1.5: Unlocking multimodal understanding across millions of tokens  
 541 of context. *arXiv preprint arXiv:2403.05530*, 2024.

542

543 Saihui Hou, Yushan Feng, and Zilei Wang. VegFru: A domain-specific dataset for fine-grained visual  
 544 categorization. In *Proc. IEEE Int. Conf. Comp. Vis.*, pp. 541–549, 2017.

545

546 Drew A Hudson and Christopher D Manning. GQA: A new dataset for real-world visual reasoning and  
 547 compositional question answering. In *Proc. IEEE Conf. Comp. Vis. Patt. Recogn.*, pp. 6700–6709,  
 548 2019.

549

550 Dong Jing, Xiaolong He, Yutian Luo, Nanyi Fei, Guoxing Yang, Wei Wei, Huiwen Zhao, and Zhiwu  
 551 Lu. FineCLIP: Self-distilled region-based clip for better fine-grained understanding. In *Advances  
 552 in Neural Inf. Process. Syst.*, pp. 27896–27918, 2024a.

553

554 Yinuo Jing, Ruxu Zhang, Kongming Liang, Yongxiang Li, Zhongjiang He, Zhanyu Ma, and Jun Guo.  
 555 Animal-Bench: Benchmarking multimodal video models for animal-centric video understanding.  
 556 In *Advances in Neural Inf. Process. Syst.*, pp. 23457–23469, 2024b.

557

558 A. Khosla, N. Jayadevaprakash, B. Yao, and L. Fei-Fei. Novel dataset for fine-grained image  
 559 categorization. In *CVPR Workshop on Fine-Grained Visual Categorization*, pp. 806–813, 2011.

560

561 Jonathan Krause, Michael Stark, Jia Deng, and Li Fei-Fei. 3D object representations for fine-grained  
 562 categorization. In *Proc. IEEE Int. Conf. Comp. Vis.*, pp. 554–561, 2013.

563

564 Alex Krizhevsky and Geoffrey Hinton. Learning multiple layers of features from tiny images.  
 565 Technical report, Citeseer, 2009.

566

567 Junnan Li, Dongxu Li, Caiming Xiong, and Steven Hoi. BLIP: Bootstrapping language-image  
 568 pre-training for unified vision-language understanding and generation. In *Proc. Int. Conf. Mach.  
 569 Learn.*, pp. 12888–12900, 2022.

570

571 Junnan Li, Dongxu Li, Silvio Savarese, and Steven Hoi. BLIP-2: Bootstrapping language-image  
 572 pre-training with frozen image encoders and large language models. In *Proc. Int. Conf. Mach.  
 573 Learn.*, pp. 19730–19742, 2023.

574

575 Dichao Liu. Progressive multi-task anti-noise learning and distilling frameworks for fine-grained  
 576 vehicle recognition. *IEEE Trans. Intell. Transp. Syst.*, 25(9):10667–10678, 2024. doi: 10.1109/  
 577 TITS.2024.3420151.

578

579 Haotian Liu, Chunyuan Li, Yuheng Li, and Yong Jae Lee. Improved baselines with visual instruction  
 580 tuning. In *Proc. IEEE Conf. Comp. Vis. Patt. Recogn.*, pp. 26296–26306, 2024a.

581

582 Yuliang Liu, Zhang Li, Mingxin Huang, Biao Yang, Wenwen Yu, Chunyuan Li, Xu-Cheng Yin, Cheng-  
 583 Lin Liu, Lianwen Jin, and Xiang Bai. OCRBench: On the hidden mystery of ocr in large multimodal  
 584 models. *Science China Information Sciences*, 67(12), 2024b. ISSN 1869-1919. doi: 10.1007/  
 585 s11432-024-4235-6. URL <http://dx.doi.org/10.1007/s11432-024-4235-6>.

586

587 Ziwei Liu, Ping Luo, Shi Qiu, Xiaogang Wang, and Xiaoou Tang. DeepFashion: Powering robust  
 588 clothes recognition and retrieval with rich annotations. In *Proc. IEEE Conf. Comp. Vis. Patt.  
 589 Recogn.*, pp. 1096–1104, 2016.

590

591 Pan Lu, Hritik Bansal, Tony Xia, Jiacheng Liu, Chunyuan Li, Hannaneh Hajishirzi, Hao Cheng,  
 592 Kai-Wei Chang, Michel Galley, and Jianfeng Gao. MathVista: Evaluating mathematical reasoning  
 593 of foundation models in visual contexts. In *Proc. Int. Conf. Learn. Representations*, 2024.

594

595 Aleksander Madry, Aleksandar Makelov, Ludwig Schmidt, Dimitris Tsipras, and Adrian Vladu.  
 596 Towards deep learning models resistant to adversarial attacks. In *Proc. Int. Conf. Learn. Represen-  
 597 tations*, 2018.

598

599 Subhransu Maji, Esa Rahtu, Juho Kannala, Matthew Blaschko, and Andrea Vedaldi. Fine-grained  
 600 visual classification of aircraft. *arXiv preprint arXiv:1306.5151*, 2013.

601

602 Ahmed Masry, Do Xuan Long, Jia Qing Tan, Shafiq Joty, and Enamul Hoque. ChartQA: A benchmark  
 603 for question answering about charts with visual and logical reasoning. In *Proc. Conf. Association  
 604 for Computational Linguistics*, pp. 2263–2279, 2022.

594 Minesh Mathew, Dimosthenis Karatzas, and CV Jawahar. DocVQA: A dataset for vqa on document  
 595 images. In *Proc. Winter Conf. Applications of Comp. Vis.*, pp. 2200–2209, 2021.  
 596

597 Maria-Elena Nilsback and Andrew Zisserman. Automated flower classification over a large number  
 598 of classes. In *Proc. IEEE Int. Conf. Comp. Vis.*, pp. 722–729, 2008.

599 2023 OpenAI. GPT-4 technical report. *arXiv preprint arXiv:2303.08774*, 2023.  
 600

601 Maxime Oquab, Timothée Darcet, Théo Moutakanni, Huy V. Vo, Marc Szafraniec, Vasil Khalidov,  
 602 Pierre Fernandez, Daniel Haziza, Francisco Massa, Alaaeldin El-Nouby, Russell Howes, Po-Yao  
 603 Huang, Hu Xu, Vasu Sharma, Shang-Wen Li, Wojciech Galuba, Mike Rabbat, Mido Assran, Nico-  
 604 las Ballas, Gabriel Synnaeve, Ishan Misra, Hervé Jegou, Julien Mairal, Patrick Labatut, Armand  
 605 Joulin, and Piotr Bojanowski. DINOV2: Learning robust visual features without supervision. *arXiv*  
 606 *preprint arXiv:2304.07193*, 2023.

607 Alec Radford, Jong Wook Kim, Chris Hallacy, Aditya Ramesh, Gabriel Goh, Sandhini Agar-  
 608 wal, Girish Sastry, Amanda Askell, Pamela Mishkin, Jack Clark, Gretchen Krueger, and Ilya  
 609 Sutskeverothers. Learning transferable visual models from natural language supervision. In *Proc.*  
 610 *Int. Conf. Mach. Learn.*, pp. 8748–8763, 2021.

611 Yang Shen, Xuhao Sun, Xiu-Shen Wei, Qing-Yuan Jiang, and Jian Yang. SEMICON: A learning-  
 612 to-hash solution for large-scale fine-grained image retrieval. In *Proc. Eur. Conf. Comp. Vis.*, pp.  
 613 531–548, 2022.  
 614

615 Arindam Sikdar, Yonghuai Liu, Siddhardha Kedaresetty, Yitian Zhao, Amr Ahmed, and Ardhendu  
 616 Behera. Interweaving insights: High-order feature interaction for fine-grained visual recognition.  
 617 In *Proc. IEEE Int. Conf. Comp. Vis.*, pp. 1755–1779, 2024.

618 Kaitao Song, Xiu-Shen Wei, Xiangbo Shu, Ren-Jie Song, and Jianfeng Lu. Bi-modal progressive  
 619 mask attention for fine-grained recognition. *IEEE Trans. Image Process.*, 29:7006–7018, 2020.  
 620

621 Quan Sun, Yuxin Fang, Ledell Wu, Xinlong Wang, and Yue Cao. EVA-CLIP: Improved training  
 622 techniques for clip at scale. *arXiv preprint arXiv:2303.15389*, 2023.

623 Tianchi. Bottled wine defect detection data set, 2021. URL <https://tianchi.aliyun.com/dataset/dataDetail?dataId=110147>.  
 624

626 Grant Van Horn, Elijah Cole, Sara Beery, Kimberly Wilber, Serge Belongie, and Oisin Mac Aodha.  
 627 Benchmarking representation learning for natural world image collections. In *Proc. IEEE Conf.*  
 628 *Comp. Vis. Patt. Recogn.*, pp. 12884–12893, 2021.

629 Catherine Wah, Steve Branson, Peter Welinder, Pietro Perona, and Serge Belongie. The Caltech-  
 630 UCSD birds-200-2011 dataset. Technical report, California Institute of Technology, 2011.  
 631

632 Wenhui Wang, Hangbo Bao, Li Dong, Johan Bjorck, Zhiliang Peng, Qiang Liu, Kriti Aggarwal,  
 633 Owais Khan Mohammed, Saksham Singhal, Subhajit Som, and Furu Wei. Image as a foreign  
 634 language: BEiT pretraining for vision and vision-language tasks. In *Proc. IEEE Conf. Comp. Vis.*  
 635 *Patt. Recogn.*, pp. 19175–19186, 2023.

636 Xiu-Shen Wei, Quan Cui, Lei Yang, Peng Wang, Lingqiao Liu, and Jian Yang. RPC: A large-scale  
 637 and fine-grained retail product checkout dataset. *Science China. Information Sciences*, 65(9):  
 638 197101, 2022a.  
 639

640 Xiu-Shen Wei, Yi-Zhe Song, Oisin Mac Aodha, Jianxin Wu, Yuxin Peng, Jinhui Tang, Jian Yang, and  
 641 Serge Belongie. Fine-grained image analysis with deep learning: A survey. *IEEE Trans. Pattern*  
 642 *Anal. Mach. Intell.*, 44(12):8927–8948, 2022b.

643 Xiu-Shen Wei, Hong-Tao Yu, Anqi Xu, Faen Zhang, and Yuxin Peng. MECOM: A meta-completion  
 644 network for fine-grained recognition with incomplete multi-modalities. *IEEE Trans. Image*  
 645 *Process.*, 33:3456–3469, 2024.

646 Ross Wightman. Pytorch image models. [https://github.com/rwightman/](https://github.com/rwightman/pytorch-image-models)  
 647 pytorch-image-models, 2019.

648 Tong Wu, Yinghao Xu, Ryan Po, Mengchen Zhang, Guandao Yang, Jiaqi Wang, Ziwei Liu, Dahua  
 649 Lin, and Gordon Wetzstein. FiVA: Fine-grained visual attribute dataset for text-to-image diffusion  
 650 models. In *Advances in Neural Inf. Process. Syst.*, pp. 31990–32011, 2024.

651

652 Peng Xu, Wenqi Shao, Kaipeng Zhang, Peng Gao, Shuo Liu, Meng Lei, Fanqing Meng, Siyuan  
 653 Huang, Yu Qiao, and Ping Luo. LVLM-eHub: A comprehensive evaluation benchmark for large  
 654 vision-language models. *IEEE Trans. Pattern Anal. Mach. Intell.*, 47(3):1877–1893, 2025. doi:  
 655 10.1109/TPAMI.2024.3507000.

656

657 Shu-Lin Xu, Faen Zhang, Xiu-Shen Wei, and Jianhua Wang. Dual attention networks for few-shot  
 658 fine-grained recognition. In *Proc. Conf. AAAI*, pp. 2911–2919, 2022.

659

660 Jiahui Yu, Zirui Wang, Vijay Vasudevan, Legg Yeung, Mojtaba Seyedhosseini, and Yonghui Wu.  
 661 CoCa: Contrastive captioners are image-text foundation models. *Transactions on Machine  
 Learning Research*, 2022.

662

663 Liu Yuan, Haodong Duan, Yuanhan Zhang, Bo Li, Songyang Zhang, Wangbo Zhao, Yike Yuan, Jiaqi  
 664 Wang, Conghui He, Ziwei Liu, Kai Chen, and Dahua Lin. MMBench: Is your multi-modal model  
 665 an all-around player? In *Proc. Eur. Conf. Comp. Vis.*, pp. 216–233, 2024.

666

667 Xiang Yue, Yuansheng Ni, Tianyu Zheng, Kai Zhang, Ruochi Liu, Ge Zhang, Samuel Stevens, Dongfu  
 668 Jiang, Weiming Ren, Yuxuan Sun, Cong Wei, Botao Yu, Ruibin Yuan, Renliang Sun, Ming Yin,  
 669 Boyuan Zheng, Zhenzhu Yang, Yibo Liu, Wenhao Huang, Huan Sun, Yu Su, and Wenhui Chen.  
 670 MMMU: A massive multi-discipline multimodal understanding and reasoning benchmark for  
 671 expert agi. In *Proc. IEEE Conf. Comp. Vis. Patt. Recogn.*, pp. 9556–9567, 2024.

672

673 Yifan Zhang and Junhui Hou. Fine-grained image-to-lidar contrastive distillation with visual founda-  
 674 tion models. In *Advances in Neural Inf. Process. Syst.*, pp. 25467–25489, 2024.

675

676 Yuhui Zhang, Alyssa Unell, Xiaohan Wang, Dhruba Ghosh, Yuchang Su, Ludwig Schmidt, and  
 677 Serena Yeung-Levy. Why are visually-grounded language models bad at image classification?  
 678 *arXiv preprint arXiv:2405.18415*, 2024.

679

680 Jinguo Zhu, Weiyun Wang, Zhe Chen, Zhaoyang Liu, Shenglong Ye, Lixin Gu, Yuchen Duan, Hao  
 681 Tian, Weijie Su, Jie Shao, Zhangwei Gao, Erfei Cui, Xuehui Wang, Yue Cao, Yangzhou Liu,  
 682 Xingguang Wei, Hongjie Zhang, Haomin Wang, Weiye Xu, Hao Li, Jiahao Wang, Nianchen Deng,  
 683 Songze Li, Yinan He, Tan Jiang, Jiapeng Luo, Yi Wang, Conghui He, Botian Shi, Xingcheng  
 684 Zhang, Wenqi Shao, Junjun He, Yingtong Xiong, Wenwen Qu, Peng Sun, Penglong Jiao, Han  
 685 Lv, Lijun Wu, Kaipeng Zhang, Huipeng Deng, Jiaye Ge, Kai Chen, Limin Wang, Min Dou,  
 686 Lewei Lu, Xizhou Zhu, Tong Lu, Dahua Lin, Yu Qiao, Jifeng Dai, and Wenhui Wang. Internvl3:  
 687 Exploring advanced training and test-time recipes for open-source multimodal models. *arXiv  
 688 preprint arXiv:2504.10479*, 2025.

689

690

691

692

693

694

695

696

697

698

699

700

701

702 

## A THE EVALUATION BENCHMARK

703 

### A.1 EVALUATION TASK DETAILS

704 In Section 3.1, we have described each evaluation task. Here, we provide further details. In the  
 705 Knowledge Bias Estimation task, to uncover potential knowledge biases across different fine-grained  
 706 categories, we pair each image with its corresponding fine-grained label to generate positive samples  
 707 for true/false questions. For constructing negative samples, each image is paired with a single fine-  
 708 grained label randomly selected from other subcategories within the same super-category. For each  
 709 fine-grained category, we calculate the LVLM’s accuracy on all corresponding true/false questions as  
 710 a measure of its understanding of that category’s knowledge.

711 In the cross meta-class classification task, we follow the DINOv2 (Oquab et al., 2023) method to  
 712 train the model on a unified training set where fine-grained categories from different datasets are  
 713 combined. The model is then tested on each individual dataset to evaluate its performance.

714 

### A.2 DATA CURATION

715 **Dataset** We source images for the FG-BMK benchmark from 12 fine-grained datasets. These  
 716 datasets cover a wide range of meta-classes, with different categories and sample, providing a  
 717 comprehensive assessment of LVLMs capabilities on fine-grained tasks across different domains.  
 718 Table 6 indicates their meta-classes, the amount of samples, the number of categories. For all datasets,  
 719 we construct human-oriented evaluation questions based on their test sets. We use the original labels  
 720 directly from the datasets for the machine-oriented evaluation.

721 Table 6: Details of 12 fine-grained datasets sorted by their numbers of categories. “Meta-class”  
 722 refers to a high-level categorization of the dataset. “Categories” refers to the number of fine-grained  
 723 categories. “Samples” refers to the total number of samples in each dataset.

Datasets	Meta-class	Categories	Samples
<i>Wine</i> (Tianchi, 2021)	Industrial	11	4,516
<i>DeepFashion</i> (Liu et al., 2016)	Clothes	46	18,000
<i>SkinCon</i> (Daneshjou et al., 2022)	Dermatology	48	3,866
<i>Flowers102</i> (Nilsback & Zisserman, 2008)	Flower	102	7,169
<i>Food101</i> (Bossard et al., 2014)	Food	101	101,000
<i>FGVC Aircraft</i> (Maji et al., 2013)	Aircraft	100	6,667
<i>Stanford Dogs</i> (Khosla et al., 2011)	Dog	120	20,580
<i>Stanford Cars</i> (Krause et al., 2013)	Car	196	16,185
<i>CUB-200-2011</i> (Wah et al., 2011)	Bird	200	11,788
<i>VegFru</i> (Hou et al., 2017)	Vegetable	292	146,131
<i>Products-10K</i> (Bai et al., 2020)	Retail	9,691	197,307
<i>iNat2021</i> (Van Horn et al., 2021)	Plants	10,000	2,786,843

724 **Human-oriented Question Templates** When constructing true/false, multiple-choice, short answer  
 725 questions for each task in human-oriented evaluation, we manually design several question templates  
 726 to ensure both diversity and comprehensive coverage. Figure 10 illustrates the question templates we  
 727 use for generating the tasks.

748 

## B EVALUATED MODELS

750 As shown in Table 7, we select nine widely-used open-source LVLMs, two closed-source models  
 751 (GPT-4o (OpenAI, 2023) and Gemini-2.0-flash (Gemini Team, 2024)) and one purely visual model,  
 752 each of which employs a distinctive training recipes, including variations in vision encoder, language  
 753 model, training losses and data.

754 

- **EVA-CLIP** (Sun et al., 2023) aligns visual and textual features using contrastive loss, leveraging  
 755 over 2 billion web image-text pairs and advanced optimization techniques.

756  
757  
758  
759  
760  
761  
762  
763  
764  
765  
766

**767 Question Template for Attribute Recognition Task**

**768 True/False Question:**

769 Is the wing color of the bird {color}?  
770 Is the breast pattern of the bird {pattern}?

**771 Multiple-choice Question:**

772 What is the wing color of the bird? Choose one from the following list: {options}.

**773 Question Template for Knowledge Bias Estimation Task**

**774 True/False Question:**

775 Is the species of the {meta\_class} {fine\_grained\_category}? Answer with yes or no.  
776 Does this {meta\_class} belong to the species known as {fine\_grained\_category}? Answer with yes or no.  
777 Is the {meta\_class} species in this photo a {fine\_grained\_category}? Answer with yes or no.  
778 From your observation, is the species of the {meta\_class} shown a {fine\_grained\_category}? Answer with yes  
779 or no

**780 Question Template for Hierarchical Granularity Recognition Task**

**781 True/False Question:**

782 Is the species of the {meta\_class} {fine\_grained\_category}? Answer with yes or no.  
783 Does this {meta\_class} belong to the species known as {fine\_grained\_category}? Answer with yes or no.  
784 Is the {meta\_class} species in this photo a {fine\_grained\_category}? Answer with yes or no.  
785 From your observation, is the species of the {meta\_class} shown a {fine\_grained\_category}? Answer with yes  
786 or no

**787 Multiple-choice Question:**

788 What is the species of the {meta\_class} in this image? Choose one answer from the following list: {options}.  
789 Answer the question using a single word or phrase.  
790 Can you identify the species of this {meta\_class}? Choose one answer from the following list: {options}.  
791 Answer the question using a single word or phrase.  
792 Which species does this {meta\_class} in the photo belong to? Choose one answer from the following list:  
793 {options}. Answer the question using a single word or phrase.  
794 Observing the {meta\_class} in the image, which of the following species is it? Choose one answer from the  
795 following list: {options}. Answer the question using a single word or phrase.

**796 Short Answer question:**

797 What species of the {meta\_class} is shown in the image? Directly answer with species names.  
798 Can you identify the species of this {meta\_class} from the image? Directly answer with species names.  
799 Which species does the {meta\_class} in this photo belong to? Directly answer with species names.  
800 Based on your observation, what species of the {meta\_class} is depicted? Directly answer with species names.

801  
802 Figure 10: Question templates for each task in huamn-oriented evaluation.  
803  
804  
805  
806  
807  
808  
809

810  
 811 Table 7: Configurations of the evaluated models. “DINOv2-L” is a purely visual model. “Con” stands  
 812 for the contrastive loss, “Gen” for the generative loss, “Mat” for the image-text matching loss, “Rec”  
 813 for the reconstruction loss as used in BEiT3 (Wang et al., 2023), and “Dis” for the distillation loss as  
 applied in DINOv2 (Oquab et al., 2023).

814 815 Model	816 Component		817 Loss Function				
	818 Vision Model	819 Language Model	820 Con	821 Gen	822 Mat	823 Rec	824 Dis
825 InternV3-7B	826 InternViT-L	827 Qwen2.5-7B	✓	✓	✓		✓
828 InternVL-Chat-V1.1	829 InternViT-6B	830 LLaMA2-13B	✓	✓	✓		
831 LLaVA-1.5-7B	832 CLIP-L	833 Vicuna-7B		✓			
834 Qwen2.5-VL	835 CLIP-600M	836 Qwen2.5-7B	✓	✓	✓		
837 Qwen-VL	838 Openclip-G	839 Qwen-7B		✓			
840 BLIP-2-FLAN-T5-XL	841 EVA-CLIP-G	842 FlanT5-XL	✓	✓	✓		
843 EVA02-CLIP-L	844 EVA02-L	845 CLIP-L	✓				
846 BEiT3-L-ITC	847 CLIP-L	848 CLIP-L				✓	
849 CoCa-L	850 CLIP-L	851 CLIP-L	✓	✓			
852 DINOv2-L	853 CLIP-L	854 /	✓				✓

825  
 826 • **InternVL3** (Zhu et al., 2025) adopts a unified pre-training approach over both multimodal and  
 827 pure-text data, enhanced by variable visual position encoding (V2PE) and advanced post-training  
 828 strategies for improved scalability and effectiveness.

829 • **InternVL** (Chen et al., 2024) leverages contrastive, matching, and generative losses in a multi-stage  
 830 training process, with a large-scale vision encoder and over 6 billion image-text pairs to align visual  
 831 and textual representation.

832 • **BLIP-2** (Li et al., 2023) bridges the modality gap between frozen image encoders and LLMs  
 833 using a lightweight Q-Former, leveraging contrastive, matching, and generative loss in a two-stage  
 834 pre-training process over 129 million data with fewer trainable parameters.

835 • **Qwen2.5-VL** (Bai et al., 2025) combines dynamic-resolution Vision Transformer with Window  
 836 Attention to reduce computational cost while preserving native image resolution.

837 • **Qwen-VL** (Bai et al., 2023) employs a three-stage training process with generative loss, using a  
 838 VL adapter to align visual and textual features while reducing computational cost over 1.4 billion  
 839 image-text pairs.

840 • **CoCa** (Yu et al., 2022) adopts task-specific attentional pooling to tailor visual representations for  
 841 different training objectives, applying contrastive loss to train the first half of the decoder and  
 842 generative loss to train the full decoder in an end-to-end manner over 5 billion image-text pairs.

843 • **BEiT3** (Wang et al., 2023) treats images as a foreign language, leveraging a mask-then-predict  
 844 objective over 36 million image-text pairs to unify vision and language pretraining, and introduces  
 845 a multiway transformer architecture for general-purpose modeling.

846 • **LLaVA** (Liu et al., 2024a) aligns visual and textual features using a simple MLP with generative  
 847 loss, leveraging 1.2 million GPT-4 (OpenAI, 2023) generated multimodal instruction-following  
 848 data for training.

849 • **DINOv2** (Oquab et al., 2023) uses a self-supervised learning approach, leveraging knowledge  
 850 distillation and a mask-then-predict strategy over 142 million images to train the vision encoder.

852 For all our evaluated model, we follow their official configurations to run the inference. We set the  
 853 temperature of all open-source models to 0, while keeping the default for closed-source APIs.

## 854 C HUMAN-ORIENTED EVALUATIONS

### 855 C.1 RESULTS OF HIERARCHICAL GRANULARITY RECOGNITION

856 Figure 2 shows InternVL3’s (Zhu et al., 2025) accuracy in answering true/false and multiple-choice  
 857 questions within hierarchical granularity recognition task on *CUB-200-2011* dataset. In Figure 11,  
 858 we present additional results for GPT-4o (OpenAI, 2023), Gemini-2.0-flash (Gemini Team, 2024),  
 859 Qwen2.5-VL (Bai et al., 2025), LLaVA (Liu et al., 2024a) and InternVL (Chen et al., 2024) on  
 860 *CUB-200-2011* (Wah et al., 2011) and *iNat2021* (Van Horn et al., 2021) datasets. As shown in  
 861 the experiments, the accuracy of all models decreases as the granularity becomes finer. When the

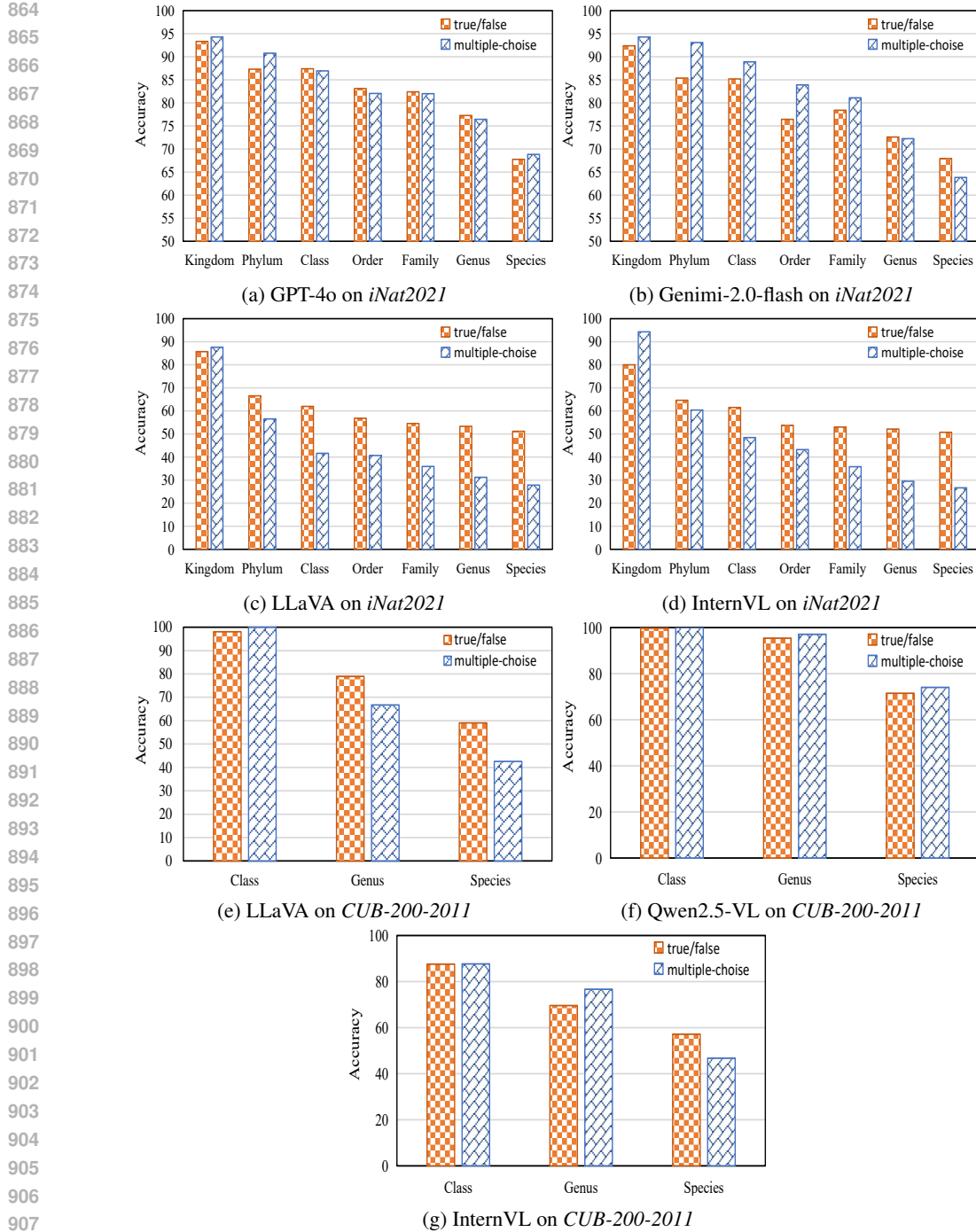


Figure 11: Results of GPT-4o (OpenAI, 2023), Gemini-2.0-flash (Gemini Team, 2024), Qwen2.5-VL (Bai et al., 2025), LLaVA (Liu et al., 2024a) and InternVL (Chen et al., 2024) on true/false and multiple-choice questions across different levels of granularity on *CUB-200-2011* (Wah et al., 2011) and *iNat2021* (Van Horn et al., 2021) dataset. The x-axis denotes the granularity of the recognition questions.

granularity level reaches the finest level, the models struggle to distinguish between closely related species.

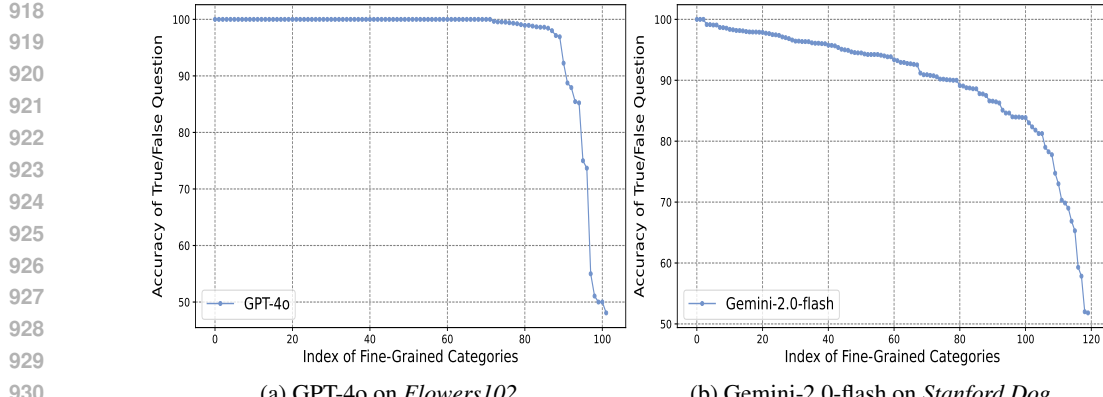


Figure 12: Knowledge bias estimation results of two closed-source models. True/false question accuracy for each category is ranked, with blue dots representing the original model.

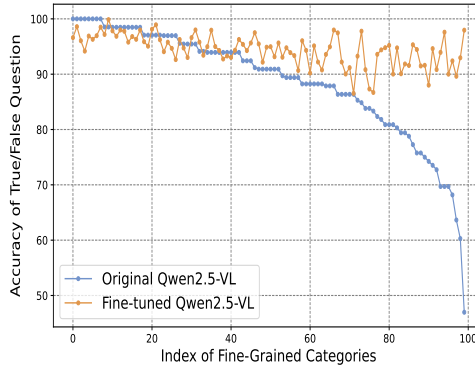


Figure 13: Comparison of the original and fine-tuned Qwen2.5-VL (Bai et al., 2025) models on occurrence-balanced fine-grained aircraft categories. True/false question accuracy for each category is ranked, with blue dots representing the original model and yellow dots representing the fine-tuned model.

## C.2 RESULTS OF KNOWLEDGE BIAS ESTIMATION

In Figure 3, we observe that LLaVA exhibit highly inconsistent recognition abilities across categories. We also conduct experiments with Qwen2.5-VL, GPT-4o, and Gemini-2.0-flash on fine-grained datasets such as Aircraft (Maji et al., 2013), Flowers102 (Nilsback & Zisserman, 2008) and Stanford Dogs (Khosla et al., 2011). As shown in Figure 12 and Figure 13, all LVLMs display similar trends, indicating inconsistent recognition abilities across fine-grained categories. However, after fine-tuned on datasets with balanced occurrences of fine-grained categories, LVLMs demonstrate remarkable recognition abilities across all fine-grained categories.

To construct datasets with balanced occurrences of fine-grained categories, we select an equal number of images from each category. Then we generate the same number of true/false questions for each fine-grained category, thereby fine-tuning the LVLMs in a way that each category receives balanced representation.

## C.3 RESULTS OF ATTRIBUTE RECOGNITION

Table 2 and Table 12 shows the attribute recognition accuracy of InternVL3 and Qwen2.5-VL on the *CUB-200-2011* dataset. The results of LLaVA, BLIP2, InternVL and Gemini-2.0-flash are shown in Table 8, Table 9, Table 10, and Table 11.

972 Table 8: Attribute recognition accuracy of LLaVA (Liu et al., 2024a) on the *CUB-200-2011* (Wah  
 973 et al., 2011) dataset (values in parentheses represent the average accuracy for each attribute).

Color Attribute (44.34)							
belly color	54.79	back color	41.90	bill color	41.44	breast color	49.56
crown color	48.71	eye color	69.27	forehead color	47.03	leg color	35.37
nape color	40.51	throat color	35.40	under tail color	38.88	underparts color	54.81
upper tail color	41.41	upperparts color	34.00	wing color	34.60	primary color	41.77
Pattern Attribute (23.69)							
back pattern	27.27	belly pattern	26.41	breast pattern	24.24	head pattern	11.35
tail pattern	23.19	wing pattern	29.67				
Shape Attribute (14.05)							
bill shape	1.39	shape	18.59	tail shape	9.89	wing shape	26.34
Length Attribute (15.71)				Size Attribute (49.47)			
bill length			15.71	size			49.47

974  
 975 Table 9: Attribute recognition accuracy of BLIP2 (Li et al., 2023) on the *CUB-200-2011* (Wah et al.,  
 976 2011) dataset (values in parentheses represent the average accuracy for each attribute).

Color Attribute (37.94)							
belly color	51.15	back color	39.64	bill color	23.42	breast color	50.17
crown color	42.59	eye color	23.59	forehead color	43.18	leg color	18.77
nape color	41.55	throat color	53.81	under tail color	37.98	underparts color	41.60
upper tail color	37.52	upperparts color	33.01	wing color	31.25	primary color	33.48
Pattern Attribute (11.34)							
back pattern	14.66	belly pattern	7.82	breast pattern	9.48	head pattern	2.14
tail pattern	14.21	wing pattern	19.73				
Shape Attribute (25.05)							
bill shape	8.84	shape	34.69	tail shape	13.51	wing shape	43.19
Length Attribute (30.11)				Size Attribute (27.62)			
bill length			30.11	size			27.62

977 Table 10: Attribute recognition accuracy of InternVL (Chen et al., 2024) on the *CUB-200-2011* (Wah  
 978 et al., 2011) dataset (values in parentheses represent the average accuracy for each attribute).

Color Attribute (35.78)							
belly color	52.09	back color	33.89	bill color	26.59	breast color	46.58
crown color	39.91	eye color	23.68	forehead color	40.83	leg color	32.75
nape color	29.66	throat color	30.21	under tail color	32.31	underparts color	50.57
upper tail color	33.42	upperparts color	29.64	wing color	27.17	primary color	40.15
Pattern Attribute (34.71)							
back pattern	35.57	belly pattern	44.14	breast pattern	42.22	head pattern	11.81
tail pattern	35.86	wing pattern	37.31				
Shape Attribute (23.03)							
bill shape	12.16	shape	38.08	tail shape	15.49	wing shape	26.43
Length Attribute (29.31)				Size Attribute (47.70)			
bill length			29.31	size			47.70

## D MACHINE-ORIENTED EVALUATIONS

### D.1 QUALITATIVE ANALYSIS OF GRANULARITY INCONSISTENCY IN LVLM ALIGNMENT DATA

1021 In the LVLM’s alignment data, we observe a phenomenon of granularity inconsistency, where fine-  
 1022 grained objects in images are paired with coarse-grained textual descriptions. Figure 14 shows some  
 1023 examples of granularity inconsistency, as well as a constructed sample of properly aligned granularity.

1024 In practice, ensuring fully consistent fine-grained granularity across all image-text pairs is often  
 1025 infeasible, especially when relying on web-scale or weakly labeled data. In our retraining experiment

1026 Table 11: Attribute recognition accuracy of Gemini-2.0-flash (Gemini Team, 2024) on the *CUB-1027*  
 1027 *200-2011* (Wah et al., 2011) dataset (values in parentheses represent the average accuracy for each  
 1028 attribute).

Color Attribute (47.22)							
belly color	62.09	back color	36.51	bill color	52.31	breast color	56.01
crown color	56.44	eye color	59.57	forehead color	53.55	leg color	40.66
nape color	40.40	throat color	60.23	under tail color	40.60	underparts color	59.65
upper tail color	39.99	upperparts color	29.66	wing color	29.21	primary color	38.69
Pattern Attribute (56.14)							
back pattern	56.26	belly pattern	70.51	breast pattern	66.89	head pattern	39.56
tail pattern	52.33	wing pattern	51.26				
Shape Attribute (48.75)							
bill shape	61.62	shape	68.20	tail shape	32.13	wing shape	33.04
Length Attribute (71.82)				Size Attribute (52.72)			
bill length		71.82		size		52.72	

1041 Table 12: Attribute recognition accuracy of Qwen2.5-VL (Bai et al., 2025) on the *CUB-200-1042*  
 1043 *2011* (Wah et al., 2011) dataset (values in parentheses represent the average accuracy for each  
 1044 attribute).

Color Attribute (40.39)							
belly color	51.11	back color	32.89	bill color	46.50	breast color	44.84
crown color	46.54	eye color	54.85	forehead color	44.57	leg color	37.79
nape color	36.49	throat color	40.74	under tail color	34.60	underparts color	50.20
upper tail color	34.92	upperparts color	27.20	wing color	26.03	primary color	36.96
Pattern Attribute (45.12)							
back pattern	42.66	belly pattern	64.58	breast pattern	59.79	head pattern	14.57
tail pattern	45.04	wing pattern	44.11				
Shape Attribute (29.30)							
bill shape	15.30	shape	58.17	tail shape	5.63	wing shape	38.10
Length Attribute (63.20)				Size Attribute (52.56)			
bill length		63.20		size		52.56	

1058 in Table 4, we made efforts to construct more consistent alignment data, but some residual mismatch  
 1059 may still exist.

1062 **D.2 IMPROVING THE FINE-GRAINED DISCRIMINABILITY OF VISUAL FEATURES DURING THE  
 1063 ALIGNMENT STAGE CAN ENHANCE LVLM PERFORMANCE ON FINE-GRAINED TASKS.**

1066 In Table 4, we can find that the alignment strategy might impair the fine-grained discriminability  
 1067 of visual features. We then conduct further analysis and find that improving the fine-grained  
 1068 discriminability of visual features during the alignment stage can enhance LVLM performance on  
 1069 fine-grained tasks.

1070 Specifically, we compare the two variants of LLaVA from Table 4 on fine-grained short-answer  
 1071 questions: (1) Vanilla LLaVA, where the vision-language alignment is trained on image-text pairs  
 1072 with granularity inconsistencies, (2) Retrained LLaVA, where the alignment module is trained on  
 1073 data with matched granularity.

1075 The results in Table 13 show that Retrained LLaVA consistently outperforms Vanilla LLaVA over  
 1076 all datasets, indicating that improving the fine-grained discriminability of visual features during the  
 1077 alignment stage can enhance LVLM performance on fine-grained tasks.

1078 Building on this finding, we believe that incorporating contrastive learning objectives (e.g., patch- or  
 1079 region-level contrastive loss) during the alignment stage may further help preserve discriminative  
 visual information.

1080

1081

1082

1083

1084

1085

1086

1087

1088

1089

1090

1091

1092

1093

1094

1095

1096

1097

1098

1099

1100

Figure 14: Qualitative analysis of granularity inconsistencies in LVLMs’ alignment data and a constructed sample of properly aligned granularity.

Table 13: Linear prob classification results of LLaVA visual features and fine-tuned results of two variants of LLaVA on fine-grained short answer questions.

Datasets	Linear			Fine-tuned	
	Origin	Aligned	Aligned-FG	Vanilla LLaVA	Retrained LLaVA
<i>CUB-200-2011</i>	79.77	73.17	75.06	85.60	86.32
<i>Stanford Dogs</i>	81.24	78.14	80.69	86.49	87.58
<i>Stanford Cars</i>	87.57	83.90	85.63	90.55	91.73
<i>Food-101</i>	94.27	93.35	94.32	95.25	95.74

1110

1111

### D.3 RESULTS OF CLASSIFICATION ACROSS MULTI-CATEGORIES

1112

In Figure 8, we have shown the classification accuracy both within a single super-category and across multiple meta-categories in three datasets. Here, in Figure 15, we include more results on nine fine-grained datasets. As shown in the results, EVA-CLIP, trained with contrastive paradigm, maintains a higher score in classification across multiple meta-categories compared to Qwen and BEiT3, which are trained with generative and reconstruction paradigms.

1113

1114

1115

1116

1117

1118

1119

1120

1121

1122

1123

1124

1125

1126

1127

1128

1129

1130

1131

1132

1133

### Qualitative Analysis of Granularity Inconsistencies in LVLMs’ Alignment Data

#### Sample1:

Question: Render a clear and concise summary of the photo.

Answer: a **cat** looking back sitting on a rock at the ocean vacation.



#### Sample2:

Question: Summarize the visual content of the image.

Answer: **dog** lying on the floor with text happy dog training can be cured by behavior experts.



#### Sample3:

Question: Describe the image concisely.

Answer: a small brown **bird** drinking water from a puddle.



#### Constructed Granularity Aligned Sample:

Question: What is the object species?

Answer: The object species is **great crested flycatcher**.



1134

1135

1136

1137

1138

1139

1140

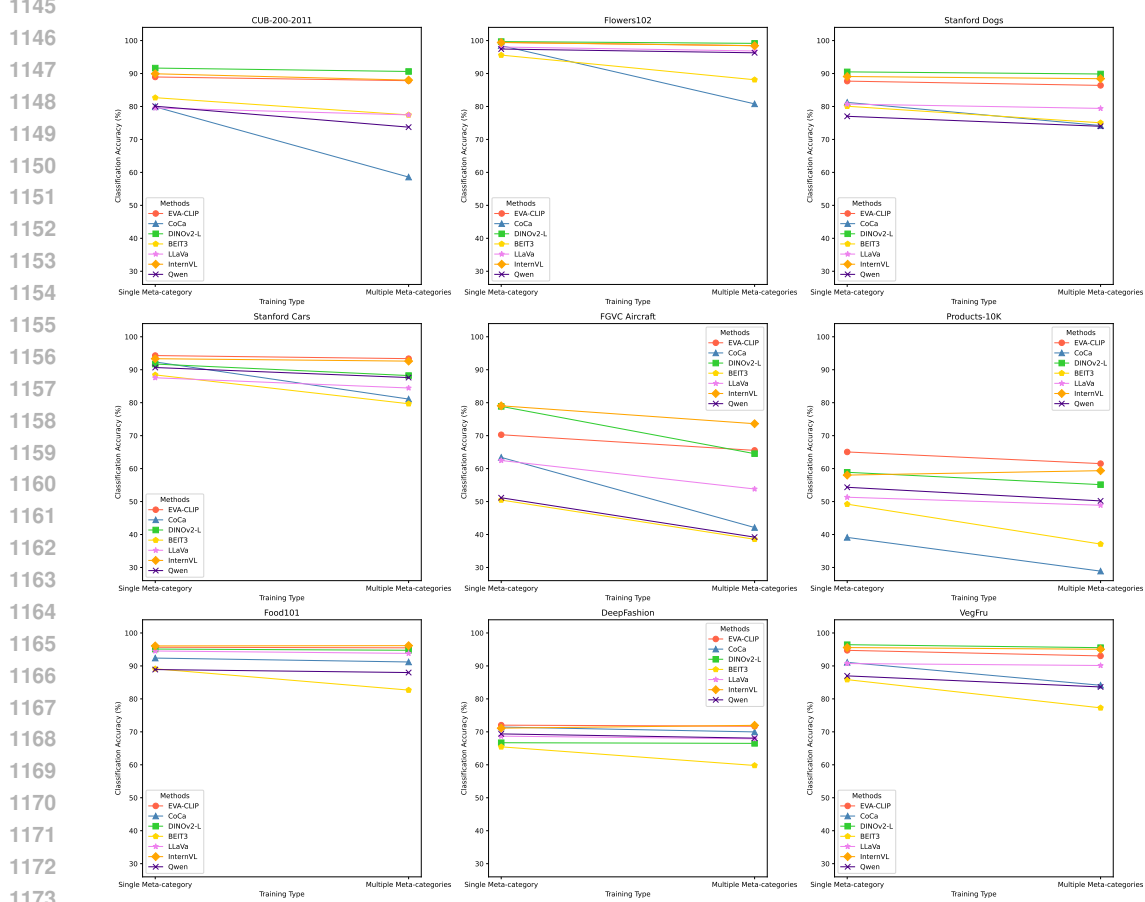
1141

1142

1143

1144

1145



1174  
1175  
1176  
1177  
1178  
1179  
1180  
1181  
1182  
1183  
1184  
1185  
1186  
1187

Figure 15: Classification results of LVLM visual features on fine-grained datasets. “Single” denotes accuracy from training on a single meta-category, while “Multiple” reflects accuracy from training on a unified dataset combining multiple meta-categories.